

# Effect of Capacitance on the Output Characteristics of Solar Cells

P. Merhej, E. Dallago, and D. Finarelli

Department of Electrical Engineering, University of Pavia, Italy

{ patrick.merhej, enrico.dallago, daniele.finarelli }@unipv.it

**Abstract**—This paper presents the capacitance effect on the output characteristics of solar cells (SCs). For this purpose, a current sweep circuit was built to bias the SC. We show that the output characteristics begin to split due to charge or discharge of the internal capacitance. Experimental results are analytically discussed and compared with simulation, employing a dynamic model of the SC implemented in Matlab environment.

**Keywords-capacitance effect; dynamic model of solar cells; maximum power point tracker.**

## I. INTRODUCTION

Silicon solar cells (SCs) capacitance is in the range of 40 nF/cm<sup>2</sup> per cell and typically SCs are treated as current source enjoying low parasitic capacitance.

In literature papers are focused on the static behavior to characterize and analyze systems employing SCs [1-3]. Few papers discuss the dynamic behavior of the SC, in [4, 5] dynamic impedance and its voltage and frequency dependence are derived, thus allowing modeling and diagnostic of a system for a photovoltaic array.

Complexity of energy production systems based on solar conversion is increasing, to enhance efficiency and output power, and increasing dynamic loads are been applied to SCs. To qualify SCs flash testing techniques (20ms) are widespread since quasi-static temperature testing can be performed [6]. To maintain the system to the maximum output power independently of external conditions, efficient SC output decoupling from actual load is performed with high frequency switching (several kHz) converters equipped with fast (0,01 s) load matching maximum power point tracker systems [7]. Dynamic behavior can be significant for measurement reliability and eventually converter stability. Non-silicon cells i.e. dye-sensitized [8], can feature large capacitance.

Computer simulations are an efficient research tool to investigate system interactions and criticalities and contribute to speculative thinking. In this paper the SC behavior is been discussed and modeled, extending a standard static SC block with the introduction of the parasitic voltage sensitive capacitance. Moreover, a first investigation on the effect of this capacitance on output characteristics is performed. Current sweep was selected as forcing bias as SCs are typically employed as current controlled sources, thus allowing complete characterization of the SC in a quasi-static temperature condition. The effect of charge and discharge of the parasitic capacitance on the output characteristic of SCs is treated. Through the dynamic model of the SC the: output

characteristic (expressed as output current as a function of output voltage) and incremental conductance are analyzed to justify the behavior of the SC. A model was built in Matlab environment to verify the phenomenon. For this purpose, the static parameters of the SC model were determined using the method developed in [9] and an estimation of the capacitance was done using the developed equation.

## II. DYNAMIC MODEL OF SC

### A. Model

The most common dynamic model of the SC, shown in fig. 1, is the single diode. It differs from the static model by adding the parallel capacitance. The elements of the equivalent circuit of the SC are explained in the following list:

- the current source, whose density is proportional to the number of free electron/hole pairs generated per second;
- the diode, which represents the p-n junction;
- the series resistance, which represents the resistance of the semiconductor material and of the metal contacts;
- the shunt resistance, which is due to the recombination losses;
- the capacitor, which embeds the transition and diffusion capacitance.

The current-voltage relationship represents the output characteristic of the dynamic model and it is given by:

$$i = I_{ph} - i_d - i_{sh} - i_c \\ = I_{ph} - I_0 \left( e^{\frac{v+R_s i}{nV_T}} - 1 \right) - \frac{v + R_s i}{R_{sh}} - c \frac{\partial(v + R_s i)}{\partial t} - (v + R_s i) \frac{\partial C_p}{\partial t} \quad (1)$$

where  $V_T$  is the thermal voltage equal to  $kT/q$  ( $k$  is the Boltzmann constant,  $q$  is the elementary charge on an electron and  $T$  is the temperature of the SC);  $I_{ph}$  is the photocurrent;  $i_d$  is the diode current and  $i_{sh}$  is the shunt current;  $v_d$  the voltage diode;  $I_0$  is the diode current saturation;  $n$  is the diode ideality factor;  $R_s$  is the series resistance;  $R_{sh}$  is the shunt resistance and  $C_p$  is the parallel capacitance.

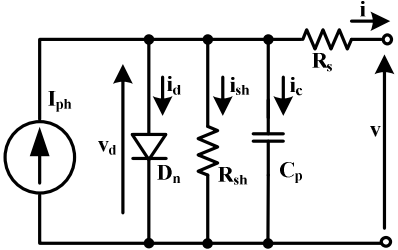


Fig. 1. Single diode SC dynamic electrical model .

At a given temperature and illumination, the five extrinsic parameters of the SC for the static model ( $I_{ph}$ ,  $I_0$ ,  $n$ ,  $R_s$ ,  $R_{sh}$ ) assume a specific value; the variation of the output characteristic depends on the applied voltage. Taking into account the dynamic effect of the SC, a separation in output voltage between rising and falling side of the current sweep is expected. This separation is also dependent on the capacitance.

### B. Capacitance estimation

Capacitance is estimated exploiting the splitting of the output characteristic due to the charge and discharge effect. The phenomenon appears to be relevant when the diode is reverse biased. For this purpose the analysis is referred to the model in reverse zone, shown in fig. 2. In this zone, the static parameters are given by the sum between the series and shunt resistance. Generally the series resistance  $R_s$  is orders of magnitude smaller than the shunt resistance therefore, for this analysis it is neglected. For a given climatic condition, the output characteristic can be expressed as:

$$i_1 = I_{ph} - \frac{v}{R_{sh}} - c \left( \frac{\partial v}{\partial t} \right)_1 - v \frac{\partial c}{\partial t}; \text{ for } \frac{\partial v}{\partial t} < 0 \quad (2)$$

$$i_2 = I_{ph} - \frac{v}{R_{sh}} - c \left( \frac{\partial v}{\partial t} \right)_2 - v \frac{\partial c}{\partial t}; \text{ for } \frac{\partial v}{\partial t} > 0 \quad (3)$$

where  $i_1$  refers to the output characteristic curve during the rising edge of the current sweep while  $i_2$  refers to the falling edge.

From (2) and (3), the capacitance can be obtained as:

$$c = \frac{i_1 - i_2}{\left( \frac{\partial v}{\partial t} \right)_2 - \left( \frac{\partial v}{\partial t} \right)_1} \quad (4)$$

As it can be seen from (4), the separation between rising and falling current sweep output characteristic is justified by the presence of the parasitic capacitance  $C_p$ .

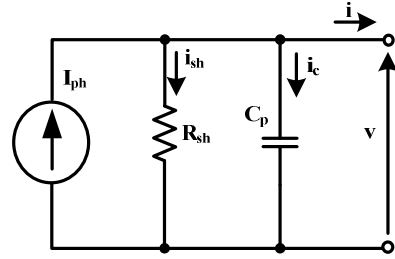


Fig. 2. SC dynamic electrical model in reverse zone.

### C. Incremental conductance.

The incremental conductance of the SC explains the different behavior of the output characteristic during rising and falling current sweep. It is defined as follows:

$$g = \frac{\partial i}{\partial v} = - \frac{\frac{1}{R_{sh}} + \frac{I_0}{nV_T} (e^{\frac{v+R_s i}{nV_T}})}{1 + R_s \frac{I_0}{nV_T} (e^{\frac{v+R_s i}{nV_T}}) + \frac{R_s}{R_{sh}} + R_s \frac{\partial c}{\partial t}} - \frac{\frac{\partial c}{\partial v} \frac{\partial(v+R_s i)}{\partial t} + c \frac{\partial^2(v+R_s i)}{\partial v \partial t} + (v+R_s i) \frac{\partial^2 c}{\partial v \partial t} + \frac{\partial c}{\partial t}}{1 + R_s \frac{I_0}{nV_T} (e^{\frac{v+R_s i}{nV_T}}) + \frac{R_s}{R_{sh}} + R_s \frac{\partial c}{\partial t}} \quad (5)$$

The effect of the capacitance is relevant for high  $\partial v / \partial t$  and the diode effect tends to cancel all terms but  $1/R_s$ . For this reason, the effect is investigated in reverse zone and the model shown in fig. 2 can be applied. In this case, the incremental conductance becomes:

$$g = \frac{\partial i}{\partial v} = - \left( \frac{1}{R_{sh}} + \frac{\partial c}{\partial v} \frac{\partial v}{\partial t} + c \frac{\partial^2 v}{\partial v \partial t} + v \frac{\partial^2 c}{\partial v \partial t} + \frac{\partial c}{\partial t} \right) \quad (6)$$

As shown in (6), incremental conductance accounts for the static term  $1/R_{sh}$  and dynamic terms, which feature opposite sign for the rising and the falling edge of the current sweep. An adequate choice of the forcing function can help recognizing the various terms involved in the dynamic component of the incremental conductance.

## III. EXPERIMENTAL RESULTS

### A. Measurement set-up

A commercial monocrystalline solar cell (125×125 mm) is used. The electrical data, under standard test conditions, are: peak power, 2,06 W;  $I_M$ , 4,33 A;  $V_M$ , 0,475 V; where  $I_M$  and  $V_M$  are the corresponding current and voltage at maximum output power, respectively. Temperature is recorded through a thermostat and the irradiance is measured using a Mac-Solar

radiation meter. The measurements were done inside laboratory and a 500 W halogen lamp was used. A function generator is used as reference for the power amplifier ( $v_{ref}$ ), which drives the SC, as shown in fig. 4. The output current is imposed through feedback of  $R_{sense}$  ( $1,62 \Omega \pm 0.01$ ). The input signal ( $v_{ref}$ ), the sensing voltage ( $v_{sense}$ ) and the amplifier output voltage ( $v_o$ ) are acquired with a digital oscilloscope (100 MHz bandwidth limited for noise rejection). This topology allows for:

- four quadrant operation using an arbitrary reference;
- fast measurement for quasi-static temperature condition on SC.
- high frequency dynamic characterization of SC through an electronic load.

### B. Experimental output characteristics

At a fixed climatic condition ( $T=26^\circ\text{C}$ ,  $G=197 \text{ W/m}^2$ ), three different measurements were done. They differ in the frequency of the bias signal. The input signal ( $V_{ref}$ ) was an ascendant/descendant ramp with a frequency equal to 0.5 kHz, 1 kHz and 2.5 kHz. From time data shown in fig. 5(a), the output characteristic ( $v-i$ ) is extracted as shown in fig. 5(b). At low frequency, the phenomenon is not relevant and the output characteristic is quasi unique (curve I). As the frequency increases, the charge and discharge effect of the capacitor becomes visible, splitting the output characteristic (curves II and III). Using the analysis developed in section II, an estimation of the capacitance was done in reverse zone. A linear dependency with the output voltage was found. The results are reported in table I for the three different cases.

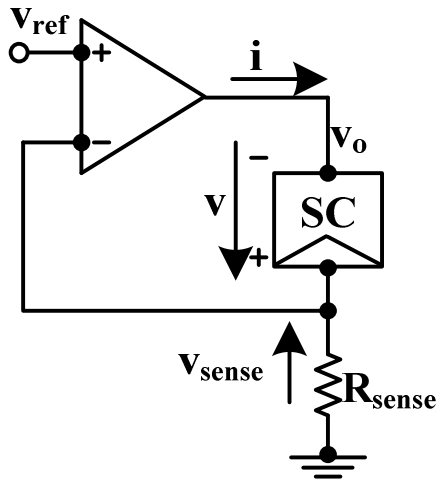


Fig. 4 Current sweep circuit.

Table I  
Capacitance estimation

Frequency [kHz]	C [ $\mu\text{F}$ ]
0,5	0,687·v+2,951
1	0,779·v+2,891
2,5	0,882·v+2,877

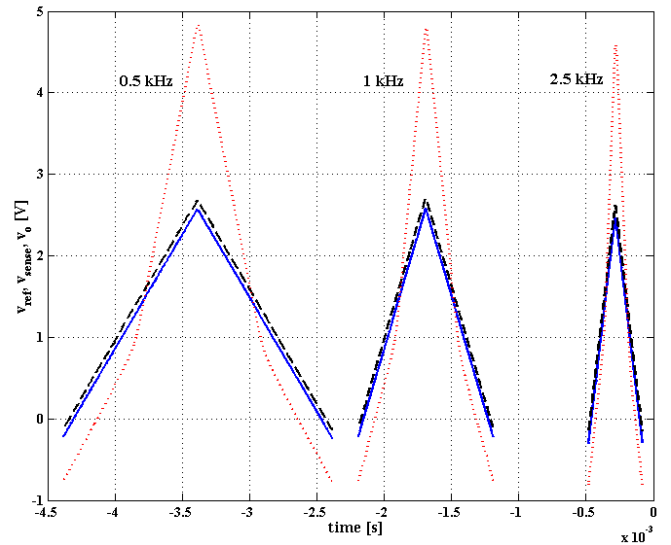


Fig. 5 (a)

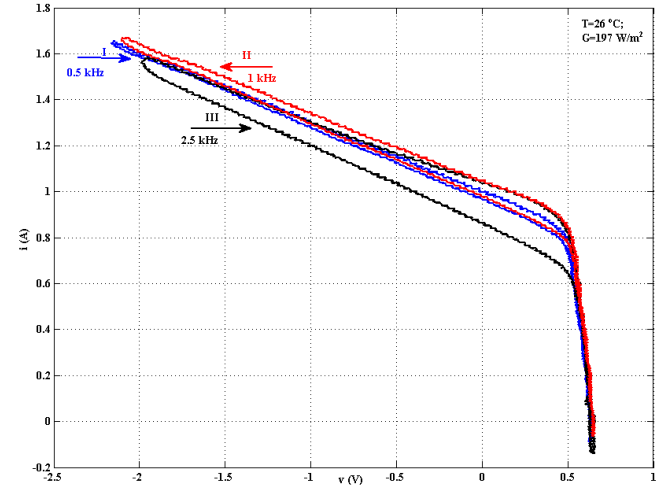


Fig. 5 (b)

Fig. 5 (a) The experimental acquired signal  $v_{ref}$  (solid line),  $v_{sense}$  (dashed line), and  $v_o$  (dotted line) in time domain; (b) Output characteristic of SC ( $v,i$ ) at three different frequency of bias (curve I at 500 Hz, curve II at 1 kHz and curve III at 2.5 kHz).

### IV. SIMULATIONS

A dynamic model of the SC was built in Matlab environment using Simulink toolbox. The evaluation of the static parameters was done and results are reported in table II. The dynamic parameter estimated in table I was used. The simulated output characteristic is obtained for a bias signal frequency of 1 kHz (fig. 6(a)) and 2.5 kHz (fig. 6(b)). In order to check the model precision, the coefficient of determination ( $R^2$ ) was calculated. It is defined as:

$$R^2 = 1 - \frac{\text{RSS}}{\text{TSS}} \quad (7)$$

Table II  
Static parameters determination (at 26 °C, 197 W/m<sup>2</sup>)

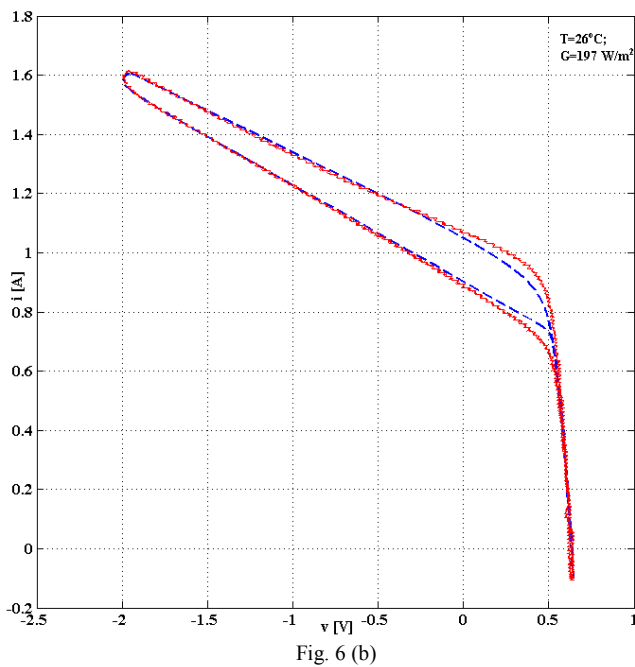
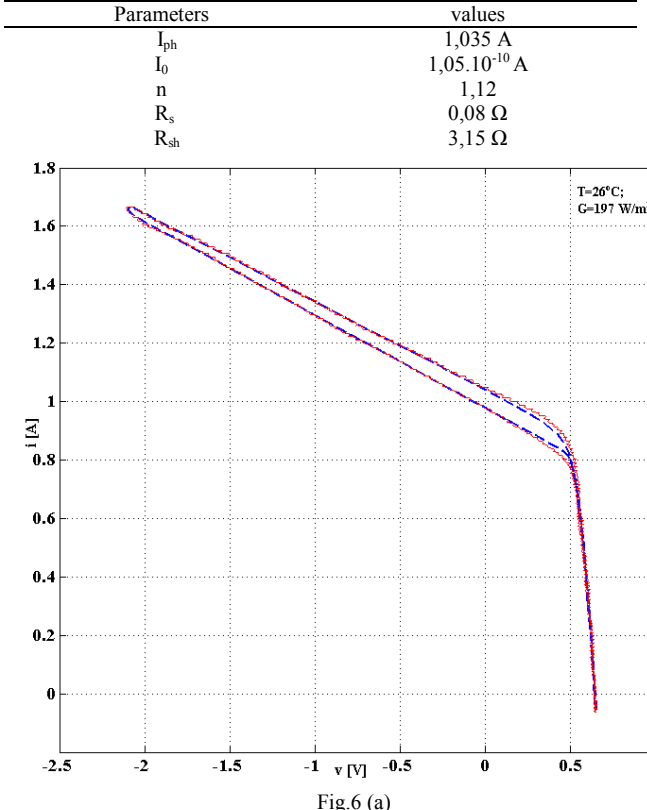


Fig 6 Experimental (solid line) and simulated (dashed line) output characteristic (a) at 1 kHz (b) at 2.5 kHz

where RSS and TSS are the residual sum of squares and the total sum of squares, respectively:

$$RSS = \sum_{i=1}^N (i_i - i_{simi-i})^2, TSS = \sum_{i=1}^N (i_i - i_m)^2 \quad (8)$$

- $i_i$  is the measured current at the  $i$ -th point among  $N$  measurements considered
- $i_{simi-i}$  is the simulated current at the same  $i$ -th point
- $i_m$  is the mean of the measured current.

For rising bias current ( $\partial v / \partial t < 0$ ), the value of  $R^2$  results 0.9969 and 0.9933 for 1 kHz and 2.5 kHz respectively while for falling bias current ( $\partial v / \partial t > 0$ ) the value of  $R^2$  results 0.9954 and 0.9936 for 1 kHz and 2.5 kHz respectively.

## V. CONCLUSIONS

The effects of the parasitic capacitance of SCs are evidenced and justified analytically. With present approximations a linear dependency with the output voltage was found. Through a Simulink model the experimental results have been replicated with good accuracy. With increasing frequency the parasitic capacitance effect extends in the diode direct bias region, eventually affecting the maximum power point.

## REFERENCES

- [1] L. Castaner, S. Silvestre, Modelling Photovoltaic Systems Using Pspice, Wiley, 2002.
- [2] J. W. Bishop, "Computer simulation of the effects of electrical mismatches in photovoltaic cell interconnection circuits," Solar Cells, Vol. 25, pp. 73–89, 1988.
- [3] J. A. Gow, C. D. Manning, "Development of a photovoltaic array model for use in power-electronics simulation studies," IEEE Proceedings of Electric Power Applications, Vol. 146, pp 193–200, March 1999
- [4] D. Chenvidhya, K. Kirtikara, C. Jivacate, "PV module dynamic impedance and its voltage and frequency dependencies," Solar Energy Materials & Solar Cells, vol 86, pp. 243–251, 2005.
- [5] J. Thongpron; K. Kirtikara, "Voltage and frequency dependent impedances of monocrystalline, polycrystalline and amorphous silicon solar cells," IEEE Photovoltaic Energy Conversion, vol. 2, pp. 2116–2119, May 2006.
- [6] W. M. Keogh, A.W. Blakers, A. Cuevas, "Constant voltage I-V curve flash tester for solar cells," Solar Energy Materials & Solar Cells, Vol 81, pp. 183–196, 2004
- [7] N. Fermia, G. Petrone, G. Spagnuolo, B, and M. Vitelli, "Optimization of perturb and observe maximum power point tracking method," IEEE Transactions on Power Electronics, Vol. 20, pp. 963–973, July 2005.
- [8] H.Tian, L. Liu, B. Liu, S.Yuan, X. Wang, Y. Wang, T. Yu, Z. Zou, Influence of capacitance characteristic on dye-sensitized solar cell's IPCE measurement," Journal of Physics, Vol. 42, 045109, 2009.
- [9] K. Bouzidi, M. Chegar, A. Bouhemadou, "Solar cells parameters evaluation considering the series and shunt resistance," Solar Energy Materials & Solar Cells ,Vol 91, pp. 1647–1651, 2007.